

Lecture 3. Intensity fluctuations and Hanbury Brown - Twiss experiment.

Intensity fluctuations. Thermal (chaotic) light. Mandel formula. Second- and higher-order correlation functions and their measurement. Hanbury Brown and Twiss experiment. Bunching and antibunching.

1. Photodetection and intensity fluctuations. Thermal (chaotic) and coherent light.

Single-mode detection. At the last lecture we discussed longitudinal and transverse modes. Suppose that we have only one mode, or our detection is single-mode (the detection volume is smaller than the coherence volume). Then our detector will be fast enough and small enough not to wipe out the intensity fluctuations.

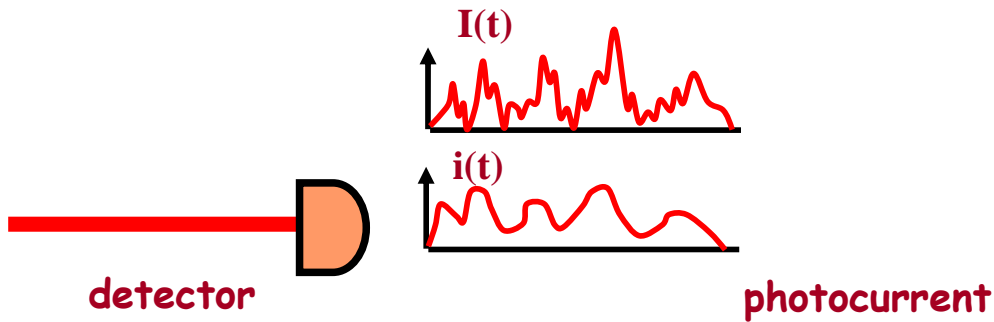


Fig.1

How it is possible to erase intensity fluctuations due to slow detection is shown in Fig.1 (analog detector, which produces photocurrent). With single photocounts, it is probably not so evident (Fig.2) but essentially the same. Anyway: the detection is single-mode if the detection time T_{det} is much smaller than the coherence time (in the figure, typical time of intensity fluctuations) and the detection area A_{det} is much smaller than the coherence area.

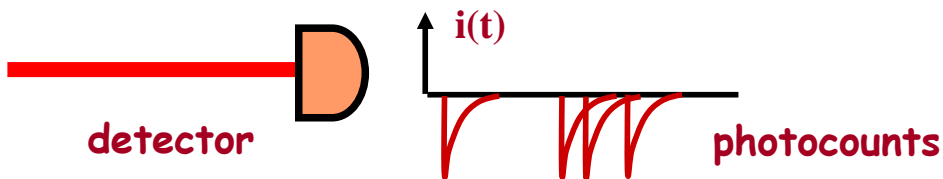


Fig.2

Provided that the detection is single-mode, one can study the statistics of light – namely, the statistics of intensity fluctuations.

Thermal (chaotic) light. The most common example of light with intensity fluctuations is light from thermal sources. Most of existing sources of light belong to this class: the Sun, the stars, gas discharge lamps, even a laser operating below threshold.

In thermal (chaotic, Gaussian) light, the field is formed by many additive independent contributions, such as different atoms emitting with independent amplitudes and phases. The result of this summation is very obvious on a phasor diagram (Fig.3).

The total analytical signal is given by the sum of many random contributions,

$$E^{(+)}(t) = \sum_i E_i^{(+)}(t).$$

According to the central limit theorem, it will have identical (but independent) Gaussian distributions of the real and imaginary parts (quadratures):

$$\text{Re}\{E^{(+)}\} \equiv X; p(X) = \frac{1}{\sqrt{2\pi}\sigma} \exp\left\{-\frac{X^2}{2\sigma^2}\right\};$$

$$\text{Im}\{E^{(+)}\} \equiv Y; p(Y) = \frac{1}{\sqrt{2\pi}\sigma} \exp\left\{-\frac{Y^2}{2\sigma^2}\right\}.$$

This is a typical probability distribution of a Gaussian complex random variable $E^{(+)}$: both real and imaginary parts are Gaussian, with the same mean values (zero) and the same standard deviation (σ). The analytical signal will be distributed as [Goodman, Statistical Optics]

$$p(E^{(+)}) = \frac{1}{\sqrt{2\pi}\sigma} \exp\left\{-\frac{X^2 + Y^2}{2\sigma^2}\right\}.$$

This distribution is shown in Fig.4. From this distribution, one can calculate separately the probability distributions for the amplitude and phase [see the Goodman book for rigorous consideration!].

The amplitude $A \equiv |E^{(+)}|$ is distributed according to the so-called Rayleigh distribution:

$$p(A) = \begin{cases} \frac{A}{\sigma^2} \exp\left\{-\frac{A^2}{2\sigma^2}\right\}, & A \geq 0, \\ 0 & \text{otherwise} \end{cases}$$

The phase is distributed uniformly between $-\pi$ and π . Note that the zero values of the amplitude are least likely. This is because what is plotted is the joint distribution of two variables, and in the centre of the picture the 'equal-phase' lines are very dense.

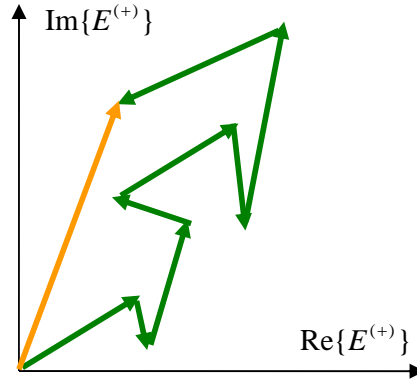


Fig.3

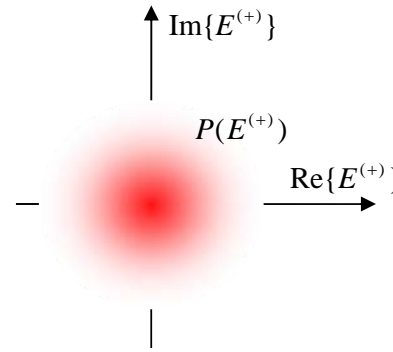


Fig.4

From the amplitude distribution, one can find the distribution of the intensity $I = A^2$:

$$p(I) = p(I = A^2) \left| \frac{dA}{dI} \right| = \frac{\sqrt{I}}{\sigma^2} \exp\left\{-\frac{I}{2\sigma^2}\right\} \frac{1}{2\sqrt{I}} = \frac{1}{2\sigma^2} \exp\left\{-\frac{I}{2\sigma^2}\right\}.$$

Thus, the intensity distribution is given by a negative exponential (most probable values are the smallest ones):

$$p(I) = \frac{1}{2\sigma^2} \exp\left\{-\frac{I}{2\sigma^2}\right\}.$$

It is convenient to express it in terms of the mean intensity, which we will now calculate (using integration by parts)

$$\langle I \rangle = \int_0^{\infty} I p(I) dI = \frac{1}{2\sigma^2} \int_0^{\infty} I \exp\left\{-\frac{I}{2\sigma^2}\right\} dI = -I \exp\left\{-\frac{I}{2\sigma^2}\right\} \Big|_0^{\infty} + \int_0^{\infty} dI \exp\left\{-\frac{I}{2\sigma^2}\right\} = 2\sigma^2.$$

Then,

$$p(I) = \frac{1}{\langle I \rangle} \exp\left\{-\frac{I}{\langle I \rangle}\right\}.$$

It is schematically shown in Fig. 5. We see that in thermal (Gaussian, chaotic) light, most probable are 'drops' of the intensity to zero and high values are least likely.

Coherent light. This is another case that can be considered classically. One can imagine a state of light with intensity fluctuations absent,
 $p(I) = \delta(I - I_0)$.

This kind of light is emitted by a laser. Intensity fluctuations in laser light are suppressed due to nonlinear-optical effect of saturation.

Further, when we pass to the quantum-optical description, we will see some quantum features of this coherent state of light. In fact, it is at the boundary between the quantum and classical ‘worlds’. The main quantum feature that will appear is the existence of fluctuations caused by the discrete photon structure, called ‘shot noise’.

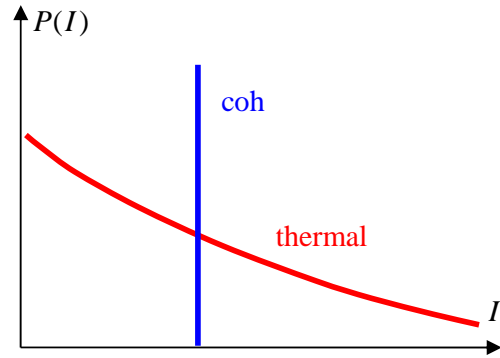


Fig.5

Arecchi's disc. Thermal light is used in many experiments, and it is convenient to make it in the lab in such a way that the coherence time is large and the coherence radius is controllable. Following the first experiments by Arecchi, it is made by placing a ground glass disc on the way of a laser beam. The transmitted light forms a speckle pattern, and the speckles move if the disc is rotated. The size of a single speckle coincides with the coherence radius and it is proportional to the inverse diameter of the beam on the disc (and to the distance, as usual). The width of the intensity distribution is inversely proportional to the size of the inhomogeneities on the disc.

2. Statistics of photocounts and Mandel's formula.

How can we study the statistics of light? For instance, if one has to distinguish between thermal and coherent light? The natural way is to study the statistics of photocurrent (Fig.1) or photocounts (Fig.2). The latter are described by the probability $p(m)$ to have a certain number m of photocounts during a sampling time T . As mentioned above, we consider the sampling time so small that the intensity I is constant within it.

Because we are so far within the framework of classical optics, light is ‘continuous’ (there are no photons!), the ‘clicks’ of a detector will appear random in time, but with a probability that scales as the intensity of light. Each ‘click’ occurs as an independent event. Then the number of ‘clicks’ within the sampling time T has a Poissonian distribution with the mean value $\langle m \rangle = \alpha I$, α depending on the quantum efficiency, sampling time T , and the detector area A_{det} :

$$p(m | I) = \frac{1}{m!} \exp\{-\alpha I\} (\alpha I)^m.$$

If the intensity fluctuates (like for the case of thermal light), then the value of I will be different from sample to sample, hence the probability distribution should be averaged over I :

$$p(m) = \int_0^{\infty} p(I) \frac{1}{m!} \exp\{-\alpha I\} (\alpha I)^m dI.$$

This equation is called the semi-classical Mandel formula. ‘Semi-classical’, because only light is considered classical here while the photocounts are described by the quantum theory (they appear due to the photoelectric effect). Further, in the part describing nonclassical light,

we will show that this semi-classical formula fails, and provide its quantum analog. Now, let us formulate some results following from the Mandel formula.

One can find any moment of the photocount number, $\langle m^k \rangle$, but it is easier to calculate the so-called *factorial moments*. A factorial moment of order k is defined as

$$G_m^{(k)} \equiv \langle m(m-1)\dots(m-k+1) \rangle = \left\langle \frac{m!}{(m-k)!} \right\rangle \equiv \sum_{m=k}^{\infty} \frac{m!}{(m-k)!} p(m).$$

Then it can be calculated through the semi-classical Mandel formula:

$$\begin{aligned} G_m^{(k)} &= \sum_{m=k}^{\infty} \frac{m!}{(m-k)!} p(m) = \sum_{m=k}^{\infty} \frac{m!}{(m-k)!} \int_0^{\infty} p(I) \frac{1}{m!} \exp\{-\alpha I\} (\alpha I)^m dI = \\ &= \int_0^{\infty} p(I) dI \exp\{-\alpha I\} (\alpha I)^k \sum_{m=k}^{\infty} \frac{1}{(m-k)!} (\alpha I)^{m-k} = \int_0^{\infty} p(I) dI \exp\{-\alpha I\} (\alpha I)^k \exp\{\alpha I\}; \end{aligned}$$

and we obtain

$$\langle m(m-k)\dots(m-k+1) \rangle = \alpha^k \langle I^k \rangle.$$

In particular, $\langle m \rangle = \alpha \langle I \rangle$ (which we already know) and

$\langle m(m-1) \rangle = \alpha^2 \langle I^2 \rangle$; then, the variance of the photocount number is

$$\Delta m^2 \equiv \langle m^2 \rangle - \langle m \rangle^2 = \alpha^2 \langle I^2 \rangle + \alpha \langle I \rangle - \alpha^2 \langle I \rangle^2 = \alpha^2 \Delta I^2 + \langle m \rangle.$$

Because the intensity should have a positive variance, we get the condition that the variance of the photocounts number should be always larger than its mean,

$$\Delta m^2 \geq \langle m \rangle.$$

In the quantum-optics part, we will see how this is violated.

For coherent light, the intensity variance is zero, hence there is the equality: $\Delta m^2 = \langle m \rangle$. So the photon-number distribution is Poissonian. For thermal light, we find (by integrating in parts) that $\Delta I^2 = \langle I \rangle^2$.

(In the quantum optics part, there will be correction to this expression when we pass from intensities to photon numbers. Namely, the shot noise will be added to this expression.)

As a result, in the case of a thermal light there are excess fluctuations of the photocount number:

$$\Delta m^2 = \langle m \rangle + \alpha^2 \langle I \rangle^2.$$

3. Hanbury Brown and Twiss interferometer. Second- and higher-order CFs and their measurement.

These excess intensity fluctuations can be observed by measuring the second-order correlation functions. In experiment, the straightforward way is to split the beam on a beamsplitter and look for correlations in the photocount number, or the photocurrents registered by analog detectors as shown in Fig.1.

Hanbury Brown and Twiss (HBT) interferometer. Using a coincidence scheme (cc) as shown in Fig.6, one can measure either the product of the photocount numbers or the product of the photocurrents. By splitting a beam, from the classical viewpoint we simply

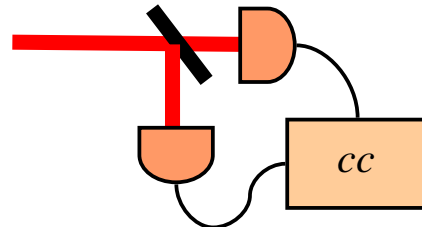


Fig.6

create its two ‘copies’. In another version, the HBT interferometer is made by simply placing two detectors at spatially separated points.

Several types of measurement, if properly performed, give the same information:

1. Mean product of photocurrents, $\langle i_1 i_2 \rangle$.
2. Mean product of photocount numbers, $\langle m_1 m_2 \rangle$.
3. Number of coincidences.

Second-order correlation functions. All these types of measurements provide the correlation function

$$G^{(2)}(t_1, t_2, r_1, r_2) \equiv \langle E^{(-)}(t_1, r_1) E^{(-)}(t_2, r_2) E^{(+)}(t_1, r_1) E^{(+)}(t_2, r_2) \rangle,$$

which is very similar to the first-order one – just has twice as many fields – and can be written as

$$G^{(2)}(t_1, t_2, r_1, r_2) \equiv \langle : I(t_1, r_1) I(t_2, r_2) : \rangle,$$

where the colons mean ‘normal ordering’ (the fact that all negative-frequency fields stand on the left and all positive-frequency fields stand on the right), and it makes sense only in quantum optics, where we will have operators instead of fields. In classical optics, all variables in the angular brackets can be interchanged.

Similarly to the first-order CFs, one can define the normalized second-order CFs:

$$g^{(2)}(t_1, t_2, r_1, r_2) \equiv \frac{\langle E^{(-)}(t_1, r_1) E^{(-)}(t_2, r_2) E^{(+)}(t_1, r_1) E^{(+)}(t_2, r_2) \rangle}{\langle E^{(-)}(t_1, r_1) E^{(+)}(t_1, r_1) \rangle \langle E^{(-)}(t_2, r_2) E^{(+)}(t_2, r_2) \rangle} = \frac{\langle : I(t_1, r_1) I(t_2, r_2) : \rangle}{\langle I(t_1, r_1) \rangle \langle I(t_2, r_2) \rangle}.$$

Higher-order CFs. Similarly, higher-order intensity CFs can be defined,

$$G^{(k)}(t_1, t_2, \dots, t_k, r_1, r_2, \dots, r_k) \equiv \langle E^{(-)}(t_1, r_1) E^{(-)}(t_2, r_2) \dots E^{(-)}(t_k, r_k) E^{(+)}(t_1, r_1) E^{(+)}(t_2, r_2) \dots E^{(+)}(t_k, r_k) \rangle,$$

and their normalized analogs,

$$g^{(k)}(t_1, t_2, \dots, t_k; r_1, r_2, \dots, r_k) \equiv \frac{\langle : I(t_1, r_1) I(t_2, r_2) \dots I(t_k, r_k) : \rangle}{\langle I(t_1, r_1) \rangle \langle I(t_2, r_2) \rangle \dots \langle I(t_k, r_k) \rangle}.$$

Of course in the stationary case the CFs depend only on the time differences and in the homogeneous case, only on the spatial displacements:

$$g^{(k)}(t_1, t_2, \dots, t_k; r_1, r_2, \dots, r_k) = g^{(k)}(t_2 - t_1, \dots, t_k - t_1; r_2 - r_1, \dots, r_k - r_1).$$

All these CFs were introduced by Glauber and are therefore called Glauber’s CFs. They can be measured by adding more detectors (with beamsplitters or without them), as shown in Fig.7.

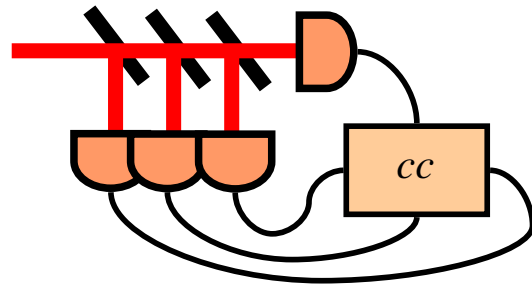


Fig.7

Second-order CFs for coherent and thermal light. One can calculate these CFs at zero delay and displacement (and therefore explain the results of Hanbury Brown and Twiss experiments) even in the classical picture. We assume that the photocurrent measured by each detector scales as the incident intensity,

$$i_{1,2} = \gamma_{1,2} I,$$

then the CF of the photocurrents is

$$\langle i_1 i_2 \rangle = \gamma_1 \gamma_2 \langle I^2 \rangle.$$

For thermal light, we can calculate (similarly to the way we calculated mean intensity) that

$$\langle I^2 \rangle = 2 \langle I \rangle^2,$$

and for coherent light,

$$\langle I^2 \rangle = \int_0^\infty dI \delta(I - I_0) I^2 = I_0^2.$$

We immediately obtain for thermal light

$$g_{th}^{(2)}(0,0) = 2$$

and for coherent light,

$$g_{coh}^{(2)}(0,0) = 1.$$

This can be generalized to the higher-order case as

$$g_{th}^{(k)}(0,0) = k!,$$

$$g_{coh}^{(k)}(0,0) = 1.$$

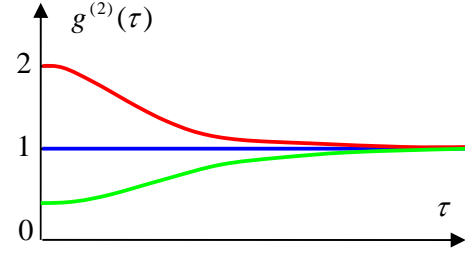


Fig.8

4. Bunching and anti-bunching.

Time (space) dependence of the second-order CF. If the time delay (or spatial displacement) is changed in the HBT interferometer, one will get a picture as shown in Fig.8. For large time

delays, intensity fluctuations are independent, hence $g^{(2)}(\infty) = 1$. For coherent light (blue

line), $g^{(2)}(\tau) = 1$ everywhere. For thermal light, $g^{(2)}(0)$ exceeds this background value, and this phenomenon is called ‘bunching’ (of photons). But you see that it can be explained without photons. It is caused just by the excess intensity fluctuations. Thermal light has them while coherent light does not.

The Siegert relation. For thermal light, there is a relation between the first- and second-order CFs. This is a consequence of the fact that for thermal light, the field is a complex Gaussian random process. As a result, second moments of the field determine all higher-order moments. In particular, there is a relation (the Siegert relation)

$$g_{th}^{(2)}(\tau, \rho) = 1 + |g_{th}^{(1)}(\tau, \rho)|^2.$$

Anti-bunching. What cannot be explained in the classical picture is the behavior shown by green line: $g^{(2)}(0) < 1$. Indeed, it contradicts the inequality derived above, $\Delta m^2 \geq \langle m \rangle$. (In the

classical picture, $g^{(2)}(0) = \frac{\langle m^2 \rangle}{\langle m \rangle^2} = \frac{\Delta m^2}{\langle m \rangle^2} + 1 \geq 1$.) This is called anti-bunching and can be

explained only within the framework of the quantum theory.

5. Stellar Hanbury Brown and Twiss interferometer

Using two spatially separated detectors, Hanbury Brown and Twiss measured the spatial second-order CFs $g_{th}^{(2)}(0, \rho)$ for several bright stars. By virtue of the Siegert relation, this measurement provides the same information as the Michelson stellar interferometer: the angular sizes of the stars. However, this measurement is much more stable as it is robust against phase fluctuations (for instance, atmospheric turbulence).

Home task:

How will the normalized second-order correlation function of the sunlight look as a function of coordinate and time if measured properly, with a single-mode detector?

Books:

1. Goodman, Statistical Optics, Section 4.2
2. Klyshko, Physical foundations of quantum electronics